

DATA REPORT

Novel *OPN1LW*/*OPN1MW* deletion mutations in 2 Japanese families with blue cone monochromacyChunxia Wang^{1,2,3,8}, Katsuhiko Hosono^{1,2,8}, Shu Kachi^{4,5}, Kimiko Suto¹, Makoto Nakamura^{4,6}, Hiroko Terasaki⁴, Yozo Miyake⁷, Yoshihiro Hotta¹ and Shinsei Minoshima²

Blue cone monochromacy (BCM) is caused by the lack of expression of the normal proteins encoded by the *OPN1LW* and *OPN1MW* genes, resulting in the absence of red and green cone sensitivities. We analyzed two cases of BCM in two different families and identified deletion mutations in the locus control region upstream of the two genes. Deletion breakpoints were determined to an accuracy of one base for both cases.

Human Genome Variation (2016) 3, 16011; doi:10.1038/hgv.2016.11; published online 26 May 2016

Blue cone monochromacy (BCM; OMIM #303700) is a rare congenital color vision disorder characterized by the absence of cone sensitivity to long (red) and medium (green) wavelengths in the retina.¹ Clinical features of BCM include severely impaired color vision and reduced visual acuity (with preservation of only rod and blue cone functions). Photophobia, myopia and congenital nystagmus are also commonly observed.²

The *OPN1LW* and *OPN1MW* genes on the X chromosome encode the red and green opsins, respectively, and are thought to be responsible for BCM.³ In the wild-type genomic array of Xq28, the genes are located head-to-tail in a tandem arrangement with a single *OPN1LW* followed by one or more *OPN1MW* copies. The actual number of *OPN1MW* copies varies among individuals. Approximately 50% of Caucasian males have two copies of *OPN1MW*s (*OPN1MW1* and *OPN1MW2*).^{1,3,4} The expression of these genes is regulated by the locus control region (LCR), a conserved sequence located upstream of the *OPN1LW* and *OPN1MW* gene cluster.⁵ The genes are encoded by six exons that show a high degree of homology (~98 and 96% identity at the nucleotide and amino acid levels, respectively).^{1,4}

BCM is caused by discrete mutations in each of *OPN1LW* and *OPN1MW* genes or a single mutation within the LCR. In 40% of BCM cases, *OPN1LW* and *OPN1MW* were inactivated by a deletion in the LCR.^{6–8} In residual cases, nonhomologous recombination between the two gene loci results in single *OPN1LW* and/or *OPN1LW*/*OPN1MW* hybrid genes carrying deleterious point mutations. The most common genotype in such cases consists of a single *OPN1LW*/*OPN1MW* hybrid gene with a c.607T > C (p.C203R) mutation in *OPN1LW*.^{8,9}

In this study, we performed a fine mutation analysis of the genomic organization at the *OPN1LW* and *OPN1MW* gene region in two Japanese families with BCM at a one base-level resolution to further understand the molecular event of the genomic deletion in the LCR.

This study was approved by the Institutional Review Board for Human Genetic and Genome Research at the Hamamatsu University School of Medicine and Nagoya University Graduate School of Medicine. All study procedures adhered to the tenets of the Declaration of Helsinki. Written informed consents were obtained from the patients of all cases before any study procedure or examination was performed.

The pedigree of family 1 is shown in Figure 1, and family 2 has been described previously.¹⁰ The characteristics of both families are consistent with an X-linked pattern of inheritance. Patients BCM1 and BCM2 are probands of families 1 and 2, respectively. Patient BCM1, an 18-year-old boy, had complained of low visual acuity since childhood. His visual acuity was 0.4 oculus dexter and 0.4 oculus sinister. Although no remarkable findings were recognized by ophthalmoscopy, BCM was strongly suspected by elaborate color vision testing and full-field electroretinography. Genomic DNA was extracted from the peripheral lymphocytes of patients using standard procedures. To identify disease-causing mutations, we performed a mutation analysis according to the following 3 steps:

- (1) PCR amplification and sequencing the amplified products for various regions of the *OPN1LW* and *OPN1MW* genes to verify their existence and to detect possible sequence alteration;
- (2) 'Junction PCR' to amplify and sequence the distant regions connected with each other after a possible large deletion for the region in which PCR amplification was unsuccessful;
- (3) Further analysis by genomic walking and cloning the unknown genomic fragments when the junction PCR was unsuccessful.

For step 1, PCR primers were designed to specifically amplify the upstream regions of the *OPN1LW* gene (accession no. NM020061; Figure 2a,b and Supplementary Table). However, designing specific primers to individually amplify each exon of *OPN1LW* and *OPN1MW* (NM_000513 for *OPN1MW1* and

¹Department of Ophthalmology, Hamamatsu University School of Medicine, Shizuoka, Japan; ²Preeminent Medical Photonics Education & Research Center, Department of Photomedical Genomics, Institute for Medical Photonics Research, Hamamatsu University School of Medicine, Shizuoka, Japan; ³Department of Ophthalmology, the 4th affiliated hospital of China Medical University, Shenyang, China; ⁴Department of Ophthalmology, Nagoya University School of Medicine, Nagoya, Japan; ⁵Matsuura eye clinic, Sakae, Ichinomiya, Japan; ⁶Nakamura eye clinic, Nagoya, Japan and ⁷Aichi Medical University, Nagakute, Japan.

Correspondence: S Minoshima (mino@hama-med.ac.jp)

⁸These authors contributed equally to this work.

Received 17 February 2016; revised 13 March 2016; accepted 1 April 2016

NM_001048181 for *OPN1MW2*) was difficult owing to the extremely high homology between these genes. Thus we designed common primers for each of the exons and employed

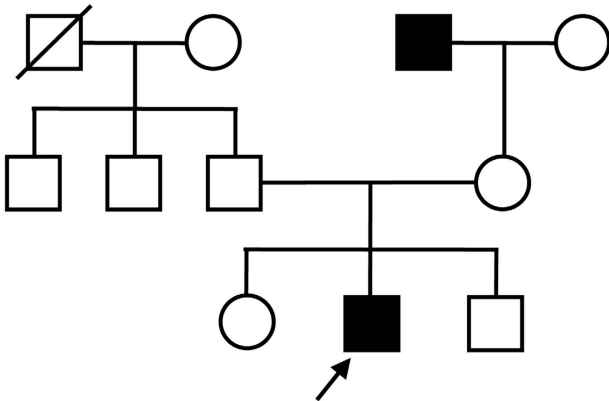


Figure 1. Pedigree of family 1. Square boxes and circles denote male and female members, respectively; black symbols indicate affected individuals; and slashed symbols indicate deceased individuals. The proband is indicated by an arrow.

them to co-amplify the exons from the genes. Only 3 exons (exons 2, 4 and 5) were selected because these could be distinguished by sequencing the amplified products (Figure 2a,b and Supplementary Table). A standard protocol¹¹ was used for the direct sequencing. Step 2 was performed in cases when the PCR products were not amplified from patients' DNA, suggesting that the genomic region concerned did not exist in the patient. After detecting large deletions and narrowing down the region by PCR and sequencing, junction PCR was performed using specific primer pairs designed to span the deletion that would work only when a deletion existed (Figure 2c,d). Step 3 involved PCR-based genomic walking using the GenomeWalker Universal kit (Takara Bio, Otsu, Japan). This kit was used according to the manufacturer's instructions to determine the unknown DNA sequence.

In the first step of the analysis of the two BCM cases, small-scale mutations such as a point mutation or a deletion/insertion of a few bases in the *OPN1LW* and *OPN1MW*s genes, and their upstream regions (including the LCR) were not detected, but long genomic deletions were suggested in both cases by the failure of PCR amplification using several primer sets (Figure 2c). The approximate deletion sizes were 20 kb in BCM1 and 41 kb in BCM2 (Figure 2c). We therefore proceeded to step 2. The junction

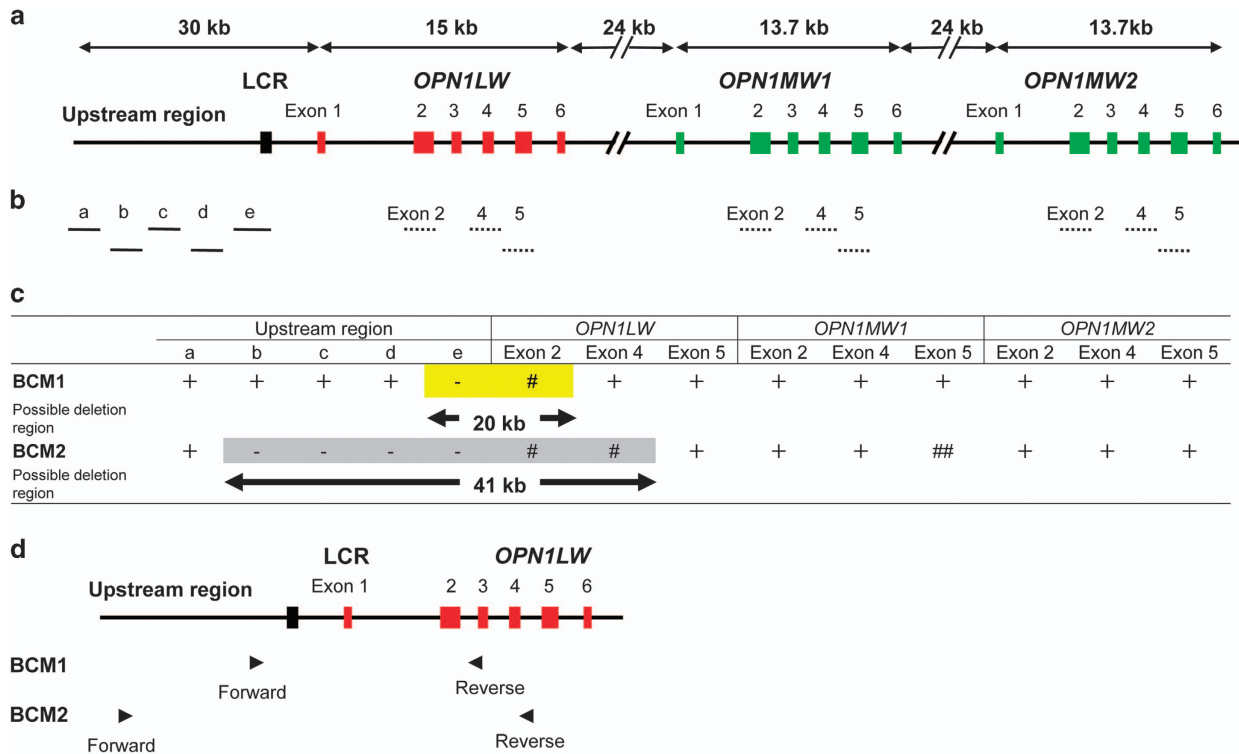


Figure 2. Gross determination of the deletion region in two Japanese families with blue cone monochromacy (BCM). **(a)** Genome structure of human *OPN1LW* and *OPN1MW*s. Red and green boxes represent *OPN1LW* and *OPN1MW*s exons, respectively; the black box represents the locus control region (LCR). **(b)** Target positions for examining the existence of each region; solid and broken lines represent unique and coexisting genomic regions, respectively. Each line was drawn along the same scale and position with the upper panel (Figure 2a). Exons 2, 4 and 5 were examined because they differ between *OPN1LW* and *OPN1MW*s. Furthermore, only exon 5 could be distinguished between *OPN1MW1* and *OPN1MW2*. Because other exons (exons 1, 3 and 6) had the same sequence in these genes, they were only examined for possible small-scale sequence alterations, including point mutations (Supplementary Table). No such mutations were detected (see text). **(c)** Summary of PCR analysis of each region. +, PCR product was amplified from patients' DNA and confirmed as *OPN1LW* or *OPN1MW*; -, PCR product was not amplified from patients' DNA; #, PCR product was amplified from patients' DNA, but sequences representing *OPN1LW* exons were absent; ##, PCR product was amplified from patients' DNA, but sequences representing the *OPN1MW1* exon was absent. In BCM1, the deletion size was estimated to be ~20 kb (yellow background). In BCM2, the deletion size was estimated to be 41 kb (gray background). The existence of exons 2 and 4 of *OPN1MW1* and/or *OPN1MW2* as well as exon 5 of *OPN1LW* and *OPN1MW2* suggested an additional complicated genomic rearrangement (see text). **(d)** Primer positions for junction PCR. Genomic structure of human *OPN1LW*. Red and black boxes represent *OPN1LW* exons and LCR, respectively. Solid arrowheads indicate forward and reverse primers used for junction PCR. The primers had the following sequences: BCM1, 5'-CACATGCGGGTGCCTACTACA-3' and 5'-TCCTATGGGGAGAGCAGAC-3'; and BCM2, 5'-CTGCCTGAAGAGAGAGGCT-3' and 5'-GACCCAGGCATAGGGAGTTG-3'.

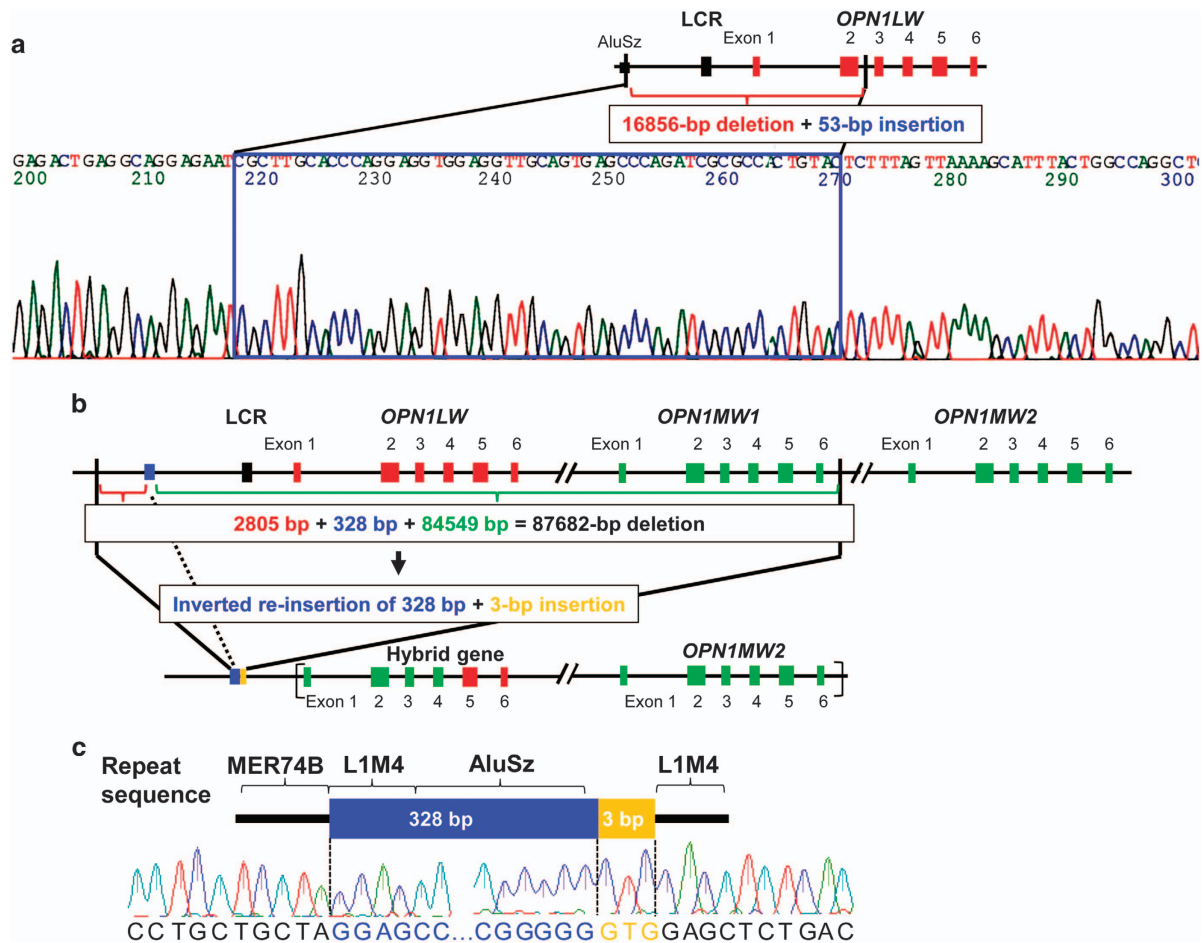


Figure 3. Determination of the region surrounding the deletion breakpoints in two Japanese families with blue cone monochromacy (BCM). **(a)** Precise analysis of the deletion–insertion mutation by junction PCR and sequencing in case BCM1. Genomic structure of human *OPN1LW*. The red and black boxes represent *OPN1LW* exons and locus control region (LCR), respectively. BCM1 had a 16,856-bp deletion and 53-bp insertion. The proximal and distal boundaries of the deletion were 8,899 bp upstream of the *OPN1LW* translation initiation codon and within *OPN1LW* intron 2, respectively. The proximal boundary of the breakpoint was an AluSz repeat sequence, and the 53-bp insertion contained a partial Alu repeat sequence. **(b)** Precise analysis of the deletion–inversion–insertion mutation by genomic walking in case BCM2. Genomic structure of human *OPN1LW* and *OPN1MW*. Red and green boxes represent *OPN1LW* and *OPN1MW* exons, respectively; the black box represents the LCR. BCM2 had an 87,682-bp deletion, an inverted re-insertion of 328 bp that is a part of the deleted sequence and a 3-bp insertion. The proximal and distal boundaries of the deletion were 28,144 bp upstream of the *OPN1LW* initiation codon and 7764 bp downstream of the *OPN1MW1* translation termination codon, respectively. In BCM2, exons 2 and 4 of *OPN1LW* were absent, whereas the presence of exon 5 in *OPN1LW* and *OPN1MW2* were confirmed. It is possible that BCM2 harbored a normal *OPN1MW2* as well as a hybrid gene comprising *OPN1MW2* exons 1–4 joined to *OPN1LW* exons 5 and 6. The brackets indicate that this structure is one of possibilities including the order of the hybrid gene and *OPN1MW2*. **(c)** Diagram and electropherogram of the region surrounding deletion–inversion–insertion breakpoints in BCM2, which were located within highly repetitive sequences.

PCR successfully identified the deletion breakpoint for BCM1, and the amplified PCR product was sequenced. We located the breakpoints as well as a 16,856-bp deletion and 53-bp insertion (5′-CGCTTGACCCAGGAGGTGGAGGTTGCAGTGAGCCAGATCGCGCCACTGTAC-3′) (Figure 3a). The proximal boundary of the deletion was 8,899 bp upstream of the *OPN1LW* translation initiation codon, and the distal boundary was 1,290 bp downstream of *OPN1LW* exon 2. We propose that this mutation be annotated as ‘c.-8899_IVS2+1290delins53 of *OPN1LW*’. Interestingly, the proximal boundary of the breakpoint was within an AluSz repeat sequence, and the 53-bp insertion was a partial Alu repeat sequence.

In the case of BCM2, the above-described method of determining the deletion region was unsuccessful, and the junction PCR primers failed to amplify a product. We hypothesized that this was due to the presence not only of a deletion but also an insertion of

unknown sequence in this region. We therefore proceeded to step 3 and performed genomic walking to identify the unknown insertion sequence. We then isolated a DNA fragment that was rich in highly repetitive sequences, including AluSz (Figure 3b,c). BCM2 harbored a complex mutation with an 87,682-bp deletion, an inverted re-insertion of 328 bp that was a part of the deleted sequence and a 3-bp (GTG) insertion. The proximal and distal boundaries of the deletion were 28,144 bp upstream of the *OPN1LW* initiation codon and 7,764 bp downstream of the *OPN1MW1* translation stop codon, respectively. The 328-bp inversion sequence was located adjacent to and downstream of the breakpoint 25,012–25,339 bp upstream of the *OPN1LW* translation initiation codon. The 3-bp (GTG) insertion was adjacent to and downstream of the inverted re-insertion. We defined the overall mutation notation as c.-28144_-25340del-25339_-25012inv328insGTG-25011_*7764del84549 of *OPN1LW/OPN1MW1*

in this study. The proximal and distal breakpoints were within the MER74B and L1M4 repetitive sequences, and the 328-bp inversion sequence included L1M4 and AluSz (Figure 3c). In BCM2, exons 2 and 4 of *OPN1LW* were absent, whereas exon 5 of *OPN1LW* and *OPN1MW2* were identified (see Figure 2 legend). This might suggest that BCM2 had normal *OPN1MW2* but also a hybrid gene comprising *OPN1MW2* exons 1–4 joined to *OPN1LW* exons 5 and 6. A possible genomic organization of BCM2 is shown in Figure 3b.

Thus, these 2 cases of BCM harbored large deletions including the LCR, but the most common mutation p.C203R was not detected. The two cases differed in terms of size and detailed features of the deletion. Because the LCR and the upstream region of the *OPN1LW* transcription site are involved in the regulation of *OPN1LW* and *OPN1MW* expression,⁵ deletion of these regions would result in the loss of red and green opsin expression, respectively. We therefore speculate that the cone photoreceptor outer segments in the two families did not express red and green opsins. Both deletions were associated with the AluSz repeat sequence in the two families (Figure 3). It was recently reported that 2 unrelated families with BCM had a complex 3-kb deletion mutation that included the LCR and insertion of an additional aberrant *OPN1MW*. The deletion–insertion breakpoints were located within 2 Alu repeat sequences (AluSx and AluSx1),¹² suggesting the involvement of highly repetitive sequences in deletion events. For the two patients in the present study, segregation analysis was not carried out due to difficulties in collecting samples from the families.

In conclusion, the disease-causing mutation in two Japanese families with BCM was a long deletion that included the LCR. This is the first single base-level mutation analysis of Japanese BCM cases caused by a deletion that includes the LCR.

HGV DATABASE

The relevant data from this Data Report are hosted at the Human Genome Variation Database at <http://dx.doi.org/10.6084/m9.figshare.hgv.799>, <http://dx.doi.org/10.6084/m9.figshare.hgv.802>.

ACKNOWLEDGEMENTS

We thank the patients who participated in this study. This work was supported by a Japan Society for the Promotion of Science Grant-in-Aid for Scientific Research (B) (no. 17390468 to SM) and Grant-in Aid for Young Scientists (B) (no. 19791261 to CW).

Supplementary Information for this article can be found on the Human Genome Variation website (<http://www.nature.com/hgv>)

COMPETING INTERESTS

The authors declare no conflict of interest.

REFERENCES

- Nathans J, Piantanida TP, Eddy RL, Shows TB, Hogness DS. Molecular genetics of inherited variation in human color vision. *Science* 1986; **232**: 203–210.
- Berson EL, Sandberg MA, Rosner B, Sullivan PL. Color plates to help identify patients with blue cone monochromatism. *Am J Ophthalmol* 1983; **95**: 741–747.
- Nathans J, Davenport CM, Maumenee IH, Lewis RA, Hejtmancik JF, Litt M *et al*. Molecular genetics of human blue cone monochromacy. *Science* 1989; **245**: 831–838.
- Nathans J, Thomas D, Hogness DS. Molecular genetics of human color vision: the genes encoding blue, green, and red pigments. *Science* 1986; **232**: 193–202.
- Wang Y, Macke JP, Merbs SL, Zack DJ, Klaunberg B, Bennett J *et al*. A locus control region adjacent to the human red and green visual pigment genes. *Neuron* 1992; **9**: 429–440.
- Ayyagari R, Kakuk LE, Coats CL, Bingham EL, Toda Y, Felius J *et al*. Bilateral macular atrophy in blue cone monochromacy (BCM) with loss of the locus control region (LCR) and part of the red pigment gene. *Mol Vis* 1999; **5**: 13.
- Ayyagari R, Kakuk LE, Bingham EL, Szczesny JJ, Kemp J, Toda Y *et al*. Spectrum of color gene deletions and phenotype in patients with blue cone monochromacy. *Hum Genet* 2000; **107**: 75–82.
- Nathans J, Maumenee IH, Zrenner E, Sadowski B, Sharpe LT, Lewis RA *et al*. Genetic heterogeneity among blue-cone monochromats. *Am J Hum Genet* 1993; **53**: 987–1000.
- Gardner JC, Michaelides M, Holder GE, Kanuga N, Webb TR, Mollon JD *et al*. Blue cone monochromacy: causative mutations and associated phenotypes. *Mol Vis* 2009; **15**: 876–884.
- Terasaki H, Miyake Y. Association of acquired color vision defects in blue cone monochromatism. *Jpn J Ophthalmol* 1995; **39**: 55–59.
- Wang C, Nakanishi N, Ohishi K, Hikoya A, Koide K, Sato M *et al*. Novel RDH5 mutation in family with mother having fundus albipunctatus and three children with retinitis pigmentosa. *Ophthalmic Genet* 2008; **29**: 29–32.
- Yatsenko SA, Bakos HA, Vitullo K, Kedrov M, Kishore A, Jennings BJ *et al*. High-resolution microarray analysis unravels complex Xq28 aberrations in patients and carriers affected by X-linked blue cone monochromacy. *Clin Genet* 2016; **89**: 82–87.



This work is licensed under a Creative Commons Attribution-NonCommercial-NoDerivs 4.0 International License. The images or other third party material in this article are included in the article's Creative Commons license, unless indicated otherwise in the credit line; if the material is not included under the Creative Commons license, users will need to obtain permission from the license holder to reproduce the material. To view a copy of this license, visit <http://creativecommons.org/licenses/by-nc-nd/4.0/>